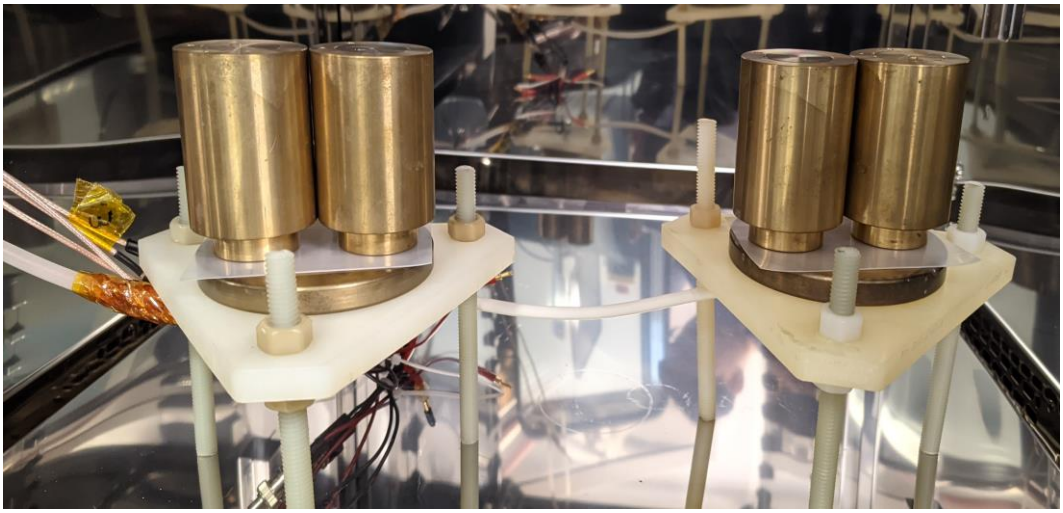

Analysis of Electric Conductivity Variance in the Insulation of HVDC Cables

Master's thesis in Electric Power Engineering

PALASH BHAUMIK

DEPARTMENT OF ELECTRICAL ENGINEERING

CHALMERS UNIVERSITY OF TECHNOLOGY
Gothenburg, Sweden 2025
www.chalmers.se

MASTER'S THESIS 2025

Analysis of Electric Conductivity Variance in the Insulation of HVDC Cables

PALASH BHAUMIK

CHALMERS
UNIVERSITY OF TECHNOLOGY

Department of Electrical Engineering
Division of Electric Power Engineering
CHALMERS UNIVERSITY OF TECHNOLOGY
Gothenburg, Sweden 2025

Analysis of Electric Conductivity Variance in the Insulation of HVDC Cables.
PALASH BHAUMIK

Supervisor: Xiangdong Xu, Research Specialist, Chalmers University of Technology
Markus Jarvid, R&D Engineer, Nexans Norway
Espen Doedens, Product and System Responsible for HVDC Extruded Cable Systems, Nexans Norway

Examiner: Yuriy Serdyuk, Professor, Chalmers University of Technology

Master's Thesis 2025
Department of Electrical Engineering
Division of Electric Power Engineering
Chalmers University of Technology
SE-412 96 Gothenburg
Telephone +46 31 772 1000

Cover: Electrical conductivity measurement setup
Typeset in LaTeX

Abstract

Power cables with insulation based on cross-linked polyethylene (XLPE) are used in high voltage direct current (HVDC) onshore and offshore power grids to transmit large amounts of electric energy over long distances. One of the important aspects to be considered when designing the insulation system of such cables is the variation of the electric conductivity of the insulation material in radial direction between the energized conductor and grounded screen. Since the conductivity of XLPE is dependent on electric field strength and temperature, predicting its actual changes in the cable is challenging and typically is done based on some empirical formulas. These, however, do not take into account the effect of the diffusion of impurities and byproducts introduced into the material during the manufacturing process on conductivity variations.

In the thesis, the electric conductivity of XLPE was measured using material samples taken from continuous peelings of the insulation of a real cable. This allowed for examining its field and temperature dependencies at different distances from the conductor, i.e. at different contents of byproducts. The experimentally obtained material properties were further utilized as input for a computer model, which was developed to analyze the dynamics of space charge accumulation and corresponding electric field in the cable. The results outlined in the thesis are essential for improving the design rules for HVDC cables to ensure their reliable and safe operation.

Acknowledgments

I would like to sincerely thank everyone who supported me during the course of this project.

I would especially like to thank my thesis supervisors from Nexans Norway, Markus Jarvid and Espen Doedens, whose technical advice and thoughtful feedback helped me stay on track and improve the quality of my work. Their insights, patience, and willingness to share their knowledge greatly impacted this project.

I would also like to thank my academic supervisor Xiangdong Xu, and examiner Yuriy Serdyuk at Chalmers University of Technology for providing me with valuable insights, support, and guidance everyday, for the entire duration of the project.

Finally, I would like to thank my parents and my sister, for being there for me as pillars of support, throughout my whole life. I wouldn't be who I am without you.

Thank you all for making this journey a meaningful and enriching one.

Gothenburg, December 2025
Palash Bhaumik

Table of Contents

1

Introduction

1.1 Background

The need for electrical energy and the continued electrification of the transportation and heating sectors grows continuously in a thriving society. Furthermore, an environmental perspective that emphasizes the need to minimize the harm to our future generations by reducing CO_2 emissions and the use of fossil fuels is also gaining traction. This necessitates the development of new, more sustainable methods for energy transmission and production. Expanding the electrical system to link more places and utilizing renewable energy sources is frequently seen as a way to reduce these rising emissions. High voltage cables become high in demand as a result, and ongoing research into better transmission systems and raising voltage levels is made easier. One effective way to deal with these upcoming issues might be through underwater HVDC cables. Extruded HVDC cables, which use crossed-linked polyethylene (XLPE) as its insulating material, and is currently a fierce rival to the conventional mass impregnated (MI) insulation system, has advanced significantly over the past few years. Higher power ratings of manufactured XLPE cables have been developed as a result of advantages like a higher rated working temperature and a quicker assembling process for its components. Despite the extensive knowledge that exists now regarding cross-linked polyethylene cables, several aspects of the cable, like the factors influencing electrical conductivity, remain unclear. Further understanding of the nature and related characteristics of this is especially necessary for the construction of HVDC transmission networks.

1.2 Research Questions

The aim of the thesis was to study the electrical conductivity in HVDC cables, by analysing the different parameters that might have an effect on it. These parameters are: temperature, humidity, electric field and presence of XLPE by-products. Out of these, only the effects of temperature and electric field were studied in this project as these are of higher significance to the industry.

Since the electrical conductivity was measured on peelings taken from the cable insulation, it was also studied if the thickness of said peelings will have an impact on the conductivity readings. Also, since the by-product content is not the same throughout the insulation after the degassing process, it was also studied if the position the peeling was taken from will have an effect on the conductivity readings.

2

Literature Review

This chapter presents the appropriate concept for this master's thesis following a thorough literature review. The two primary sections are "HVDC Cable" in section 2.1 and "Electric Conductivity of Insulating Polymers" in section 2.2. Theory pertaining to the cable's insulation is provided in the former, while information about the concept of conductivity and how it relates to insulation is provided in the latter.

2.1 HVDC Cable

2.1.1 Structure

This section will describe the major components of a typical underwater HVDC cable as well as the production process. It is important to note that every high voltage cable is made to order for a certain use and specification, making each cable distinct and one-of-a-kind. The cross section of a standard underwater HVDC cable is shown in Figure 2.1.

The different layers of the cable, and their functions are explained here:

- The section of the cable that carries the current is called the **conductor**. The conductor can be produced in a variety of designs because its shape and dimensions have been tailored to take into account the application. A copper-based cylindrical conductor is depicted in the cross-section in Figure 2.1
- The cable's **innermost semi-conductive layer** serves to evenly distribute the electric field produced by the conductor and avoid excessive strain at localized spots and protrusions, which can result in field enhancements. A

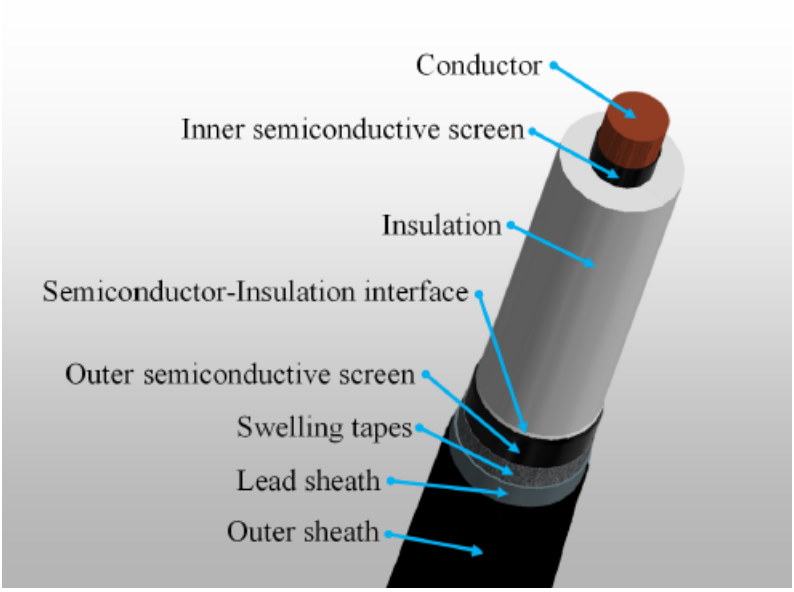

Figure 2.1: *Structure of a standard HVDC cable [2].*

semi conductive material, such as carbon black [5], is mixed with polyethylene to create this layer. Following which, the material is extruded all the way around the conductor.

- The next layer is the **insulation**, which is used to ensure an effective barrier between the grounded sheath and the conductor, which is at a higher potential. It is crucial to have an insulating material with excellent chemophysical uniformity and consistency , since the insulation is subjected to extremely large potential differences. This also has the effect of extending the insulation's lifespan, since there will be no localized hotspots in the material [6]. To maximize its resistance to aging and temperature changes, the insulation's sturdiness is also crucial. Polymers are frequently utilized for the insulation layer, with XLPE being the most frequently used material for HVDC cables [4].

- The **outermost semi-conductive layer** serves a similar purpose as the inner layer. However, here the purpose is to smoothen out the electric field near the outer part of the insulation layer. Once more, this guarantees that no local hotspots will occur, and the protrusions in the insulation will experience minimal stress. Together with the insulation and the inner semi-conductive layer, it helps the cable have reduced leakage current, which lowers the heating losses of the insulation.

- When an external damage occurs, the **swelling tapes** in the HVDC cables will stop the water from leaking into the cable [6]. A portion of the ca-

ble could become exposed to water in the event of an external mechanical fault and may fail, but the penetration of water into the rest of the cable is averted. As a result, any repairs that are needed, are unlikely to require removing large parts of the cable. Therefore, if there is any penetration of water through the outer sheath, the swelling tape should guarantee adequate water absorption and expansion [7].

- The section of the cable that serves as the exterior barrier against any water intrusion is called the **lead sheath**. Lead can be manufactured, transported, and installed as a single metallic extrusion, since it is a soft metal with a comparatively low melting point. However, extra care must be taken to avoid any mechanical damage.
- To provide strength and protection to the lead sheath positioned below it, the cable's **outer sheath** is used. Like the insulating layer, the outer sheath is often made of polymers.

Extra layers that are not shown in Figure 2.1 might consist of a number of additional protective and armoring layers that strengthen the cable and enable installations to be made even deeper. The cable is designed to support its own weight while it is being installed. This results in significant mechanical tensile strains that are mostly supported by the armoring and, to a lesser extent, by the cable's conductor layer. Given that the analysis of an extruded HVDC cable is the main goal of this thesis, a brief explanation of the triple-extrusion process of the cable shown in Figure 2.1 is required. Generally speaking, the extrusion process involves precisely balancing the production line speed, and the heating and cooling of the different layers in order to regulate the melting, chemical crosslinking, and polymeric chain relaxation processes [6]. The insulation and both the semiconductive layers are together extruded over the copper or aluminium conductor in this triple-extrusion procedure. This minimizes the effects of field enhancements, as discussed earlier, and prevents contaminants by ensuring a smooth finish over the conductor's outer interface. The cable is typically wound onto a drum or a bigger turntable following the triple extrusion process, and the entire cable is sent for the degassing process. During this process, the insulation system's chemical purity is increased to guarantee minimal leakage current, by eliminating most of the chemical cross-linking by-products. Also, methane is removed to prevent explosions.

2.1.2 Insulation

Cross-linked polyethylene (XLPE) or mass-impregnated paper are typically used as the insulation for an HVDC cable [2]. Since XLPE is the primary insulating material discussed in this thesis, this chapter first does a thorough literature review of the molecular structure of polyethylene in order to better understand how XLPE responds to electric fields.

The most common plastic made worldwide is polyethylene [8]. It is made up of

several ethylene repeat units, which are hydrocarbons with the chemical formula of C_2H_4, that combine to form a molecular chain known as a 'polymer'. The word 'polymer' is a combination of two Greek words "poly" and "meros," which mean "many" and "parts", respectively. Thus, it makes perfect sense that a polymer would be a chain of many parts; for instance, polyethylene indicates that there are numerous ethylene molecules. Two main parameters influence the polymer's mechanical characteristics [9]:

1. The number of repeat units, which, in the case of linear chain configurations, is proportional to the total polymer chain length. This is also known as relative molecular mass, or RMM for short.

2. The mechanical properties of the polymer are also significantly influenced by its overall shape.

Ethylene monomers are combined to create the polyethylene molecule. The idea is to start the processes required for chain growth by applying high, regulated pressure and temperature to a reactor containing ethylene monomers. The chemical compositions of a polyethylene chain that contains a free radical and an ethylene monomer are as follows:

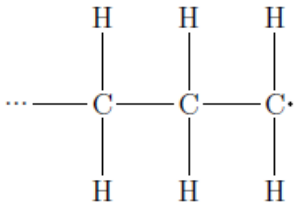

Figure 2.2: *Structure of a polyethylene chain, with a free radical*

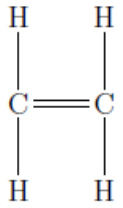

Figure 2.3: *Structure of a single ethylene monomer*

The ethylene monomer will bind to the end of the polyethylene chain (black dot in Figure 2.2) during chain expansion, opening the double bonded carbon atom.

Thus, one of the ethylene monomer's carbon atoms is completed; the other, however, still desires an additional electron and will eventually locate another ethylene monomer. In this way, ethylene monomers will continue attaching to the polyethylene molecule, which is how the polymer chain expands.

The geometry of the final polymer will vary depending on the circumstances that exist throughout the polymerization process. Cross-linked polyethylene (XLPE), high-density polyethylene (HDPE), and low-density polyethylene (LDPE) are the three most prevalent geometries of polyethylene chains [10]. Figure 2.4 shows the geometries of these polymers. The existence of what are known as "side-branches" is the primary distinction between HDPE and LDPE. These are produced when a polymer molecule captures a hydrogen atom from a nearby main chain that has already been completed (chain transfer) rather than addition of an ethylene monomer to its end. This means that the chain is now finished because the final carbon atom has all the valence electrons needed in its outermost layer. Meanwhile, the neighboring polymer chain now has an incomplete carbon atom due to the removal of a hydrogen atom, and it will try to connect with another ethylene monomer. As a result, the polyethylene chain will keep expanding, but from a different direction, as shown in Figure 2.5. This is called long side branching. Short branching results from a different process known as "chain backbiting," in which the radical shifts several places back along the original chain and proceeds to grow from the new location.

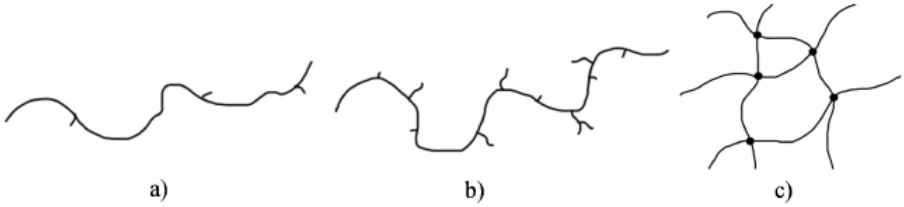

Figure 2.4: *Structure of a) HDPE chain, b) LDPE chain, c) XLPE chain [10].*

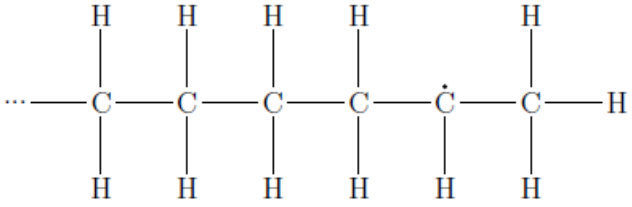

Figure 2.5: *Structure of a side branched polymer chain.*

These molecules may organize themselves within crystalline structures, called

lamellar, more tightly and orderly with lesser side branches, which raises the density of the material. If there are 3 side branches for every 100 carbon atoms in the primary chain, it is defined as LDPE [9], as a greater number of side branches results in a lower density. In contrast, HDPE is simpler to pack tightly, since it has only 1 side branch for every 100 carbon atoms, giving it the moniker "high-density polyethylene." Being the case that XLPE is cross linked, i.e. connected to a broad network of chains via many cross links, sets it apart from the other two varieties. HDPE or LDPE polymeric chains can be cross-linked through the addition of dicumyl peroxide at low temperatures, extruding the resulting mixture while it is still below the decomposition temperature, and subsequently vulcanizing it above the decomposition temperature. Free radicals are created on the polymer chains when the dicumyl peroxide breaks down and removes hydrogen atoms from them. The "cross-link" is created after two radicals on separate chains come into contact and form a covalent bond. It is generally believed that XLPE has the best mechanical qualities, such as impact and tensile strength, among these three distinct polymer chain topologies [9]. The fact that both HDPE and LDPE are thermoplastic, and XLPE is thermoset is a further significant distinction between the three polymeric topologies. The term "thermoset" refers to a polymer's fixed shape, which means that it will maintain its shape even if heated over its melting point (unless the carbon atoms' covalent connections are broken due to the excessive temperature). The opposite of thermoset is thermoplastic, which is a polymer that can be molded and shaped if heated above its melting point [11].

Another concept that can be used to further explain why HDPE packs denser than LDPE is crystallinity, which refers to the degree of molecular structure inside a material. HDPE is inherently more crystalline than LDPE, and polyethylene is somewhat crystalline at ambient temperature. Since side branching limits lamellar growth, it is generally accepted that irregular structure of molecules limits crystallinity. Also, a polymer is said to be amorphous since it is just semi-crystalline rather than completely crystalline. The Greek words "a" and "morphé," which signify "without" and "shape", respectively, are combined to form this. The non-crystalline amorphous elements of the material are metaphorically "sandwiched" between structures that look like crystal plates, which is commonly known as lamellae [11]. After heating the material to its melting point, represented by Tm, and then cooling it to a lower temperature, the material starts to crystallize [9]. After cooling to a specific temperature, polyethylene will become amorphous, and transparent, from being translucent at room temperature, and at the same time, spherulites will begin to develop. As time passes, these spherulites will expand radially after beginning their growth from a nucleus.

The crystalline structure gets destroyed when polyethylene is heated above its melting point; nevertheless, when it cools, the spherulites expand as increasing numbers of chains cling to the crystal structure. This process persists on until it comes into contact with an additional spherulite or if the polyethylene material internally contains imperfections or an impurity that prevents crystallization.

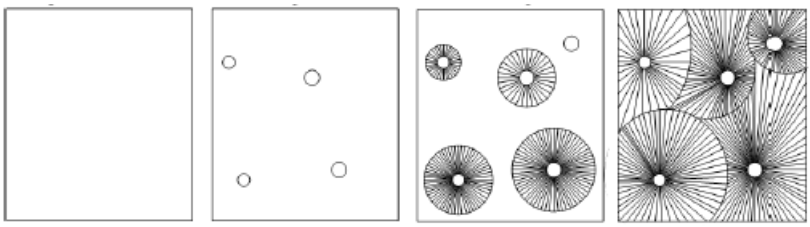

Figure 2.6: *Process of formation of spherulites [11].*

The glass transition temperature, or Tg, is another crucial temperature when talking about polyethylene, in addition to the melting temperature, or Tm. It is the temperature at which a polymer transforms from glass to liquid. A polymer is said to be in its glassy state when its main structure is immobile; when the temperature rises over Tg, the polymer transforms into a liquid state, in which the molecules are more free to move. The glass transition temperature for XLPE is significantly lower than room temperature. As a result, the material permits chain mobility under all operating parameters.

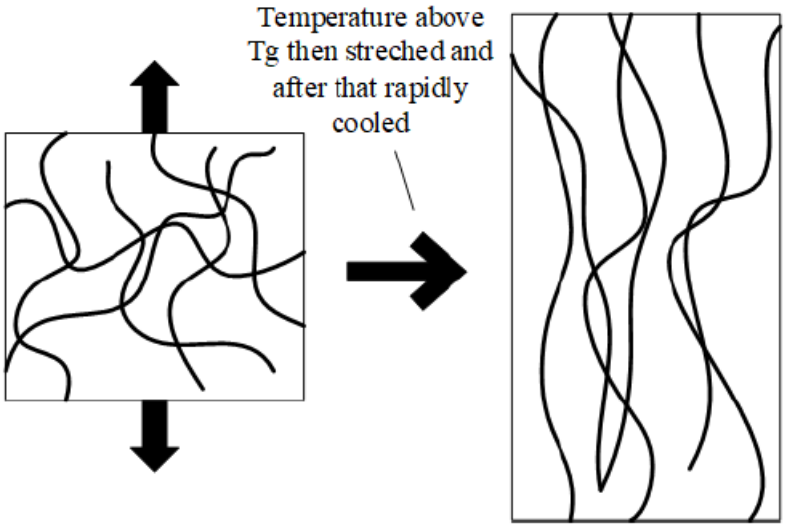

Figure 2.7: *Polymer structure changes after going through process of cable extrusion [11].*

By giving the crystalline polymer an orientated structure, its mechanical characteristics can be further enhanced [9]. Consider a number of randomly aligned

polyethylene molecules; the chains can be thought of as spaghetti. If the material is heated above the glass transition temperature (Tg) and then quickly cooled by quenching, it will acquire an orientated structure because the polymer chains will cease to be randomly oriented. Figure 2.7 illustrates this procedure. Although this method is widely used in fiber-forming, the glass transition temperature for polyethylene, as mentioned earlier, is much lower than room temperature. As a result, retaining this polymer orientation is impossible to maintain. Nevertheless, the material travels via a small opening in the extrusion head for the cable extrusion step. As a result, the polymer may have an alternate morphology (crystalline shape) after passing through the extrusion head than one made using a press-molding method. Morphology is one of the characteristics that influence an insulating polymer's electrical conductivity. In the case of semi-crystalline polymers like polyethylene, electrical conductivity often diminishes as the polymeric chain orientation increases [12].

2.2 Electric Conductivity of Insulating Polymers

Conductivity is a measure of a material's ability to conduct electric current and is the inverse of electrical resistance. Electrical conductivity can be expressed as follows:

$$\sigma = \frac{1}{\rho} = \frac{1}{R\frac{A}{l}} = \frac{J}{E} \tag{2.1}$$

with the unit of $[(\Omega m)^{-1}]$. In a nutshell, electric current is the movement of charge and is measured in Coulombs per second, also known as amperes. Diffusion and drift are the two primary modes of transportation of charges [16]. When an electric field is produced, an electrostatic force is created that causes the charge carriers to drift. The charge carriers travel as a result of diffusion because of a concentration gradient and random movement. Then conductivity can be written as follows:

$$\sigma = e \times (n\mu_n + p\mu_p) \tag{2.2}$$

$$\mu = \frac{v_d}{E} \tag{2.3}$$

where e denotes the elementary charge, n and p the concentration of electrons and holes, μ_n and μ_p the mobility of electrons and holes. v_d is the drift velocity of the charge carriers [16]. To comprehend how the idea of conductivity relates to polymers, the appropriate theory will be discussed in this part.

2.2.1 The Application of Energy Band Theory to Polymers

The Pauli exclusion principle states that two electrons cannot occupy the same space and have exactly the same energy [11]. To put it another way, every energy

state can only contain one electron. Nonetheless, the electron orbitals may partially overlap when atoms are extremely close to one another. There will be a tiny variation in energy since the electrons' energies cannot be the same. There will be many electron orbitals overlapping and a wide range of distinct energy levels when many atoms are assembled in this way to form a molecule or crystalline solid. An energy band is created by the difference between the electrons' lowest and highest energy levels; this idea is illustrated in Figure 2.8. A band gap is the area between two energy bands where there are no states (or bands) that contain electrons [16]. The valence band is at the bottom of the band gap, and the conduction band is at the top.

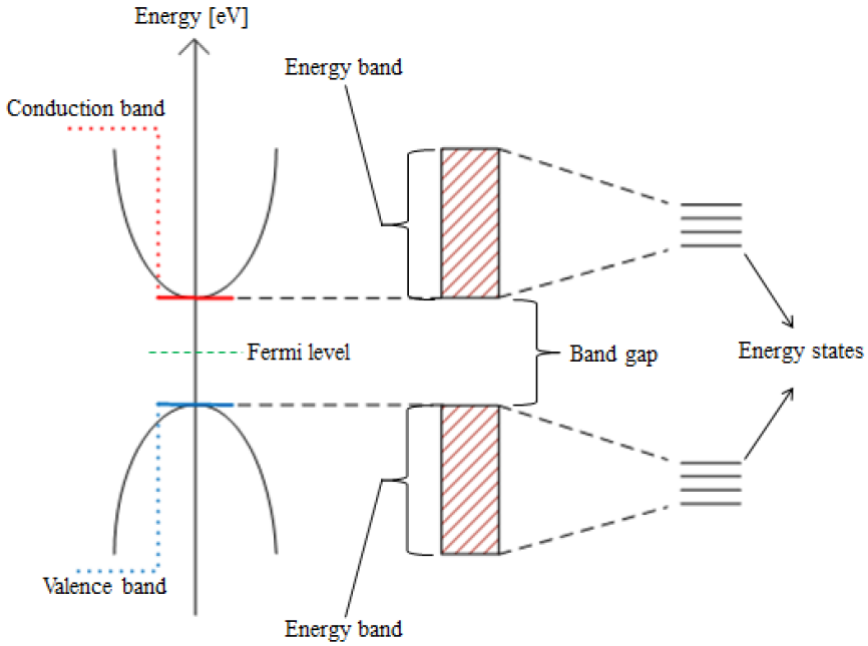

Figure 2.8: *Illustration of energy bands and band gaps. [16]*

Simply put, the band gap is the space between the top of the valence band and the bottom of the conduction band. An electron cannot gain any energy in the band gap, which implies that there are no states that might contain an electron [16]. Following the explanation of the band theory, a few pertinent words will be introduced.

- Vacuum level - this serves as a baseline for comparing different materials. It is the energy of an electron in a vacuum that is stationary.
- Ionization energy - the difference between the electron's energy level and the vacuum level is known as the ionization energy. Put differently, it is the least amount of energy needed to energize an electron to the point that it

escapes the atom or molecule, leaving behind a free electron and a positive ion.

- Fermi level - according to the Fermi-Dirac distribution function, if an electron state exists at the Fermi level, there is a 50% chance that it contains an electron [16].
- Work function - is the amount of energy required to transfer an electron from the atom's Fermi level to its vacuum level.
- Electron affinity - can be characterized by the energy released when an atom accepts an electron, creating a negative ion. It can also be defined as the energy required to extract an electron from the conduction band's lowest point.

Since an electron in the conduction band has a greater energy than the Fermi level, conduction is possible if the energy is high enough to excite an electron from the valence band to the conduction band. This will result in a hole in the valence band, which is essentially a positive charge carrier, and a missing electron. The mobility and quantity of holes and electrons, respectively, determine the conductivity, according to the equation 2.2.

A material's band gap can be used to quantify whether it is an insulator, a semiconductor, or a conductor. These are:

- Conductor - a substance that has a band gap of less than 0.2 [eV]. For instance, an energy band may only be partially filled, giving the impression that there is no energy gap.
- Semi-conductor - any substance with a band gap within 0.2 and 2.0 [eV].
- Insulator - any substance where the band gap is more than 2.0 [eV].

2.2.2 Conduction of Electrons inside the Insulation

As mentioned in the preceding section, excitation is necessary for the creation of hole and electron pairs in insulators and semiconductors, necessitating the addition of enough energy to be transferred via the energy band. A more detailed description of electronic conduction in areas where thermal energy is insufficient for excitation in the energy band will be provided in this section. It is important to note in this section that the extrusion process produces residues, which leave contaminants in the polymer and cause energy states, called traps, between molecules, and at molecular chain defects [17]. We won't address this now, but these residues can also move themselves upon ionization. Other chemical imperfections in the polymer as well as physical disorders may be the source of further traps [11]. Until enough energy is obtained, these localized states will enclose the electrons and holes, making trapped charges inaccessible for conduction.

In addition to having varying densities, the traps are positioned at various energy depths. This implies that the different potential barriers of the traps determine the energy needed for carriers to stay free and conduct in the material. It can be concluded that the movement of carriers is not caused by thermal excitation to the conduction band due to excessively high temperature levels because the potential barriers of the traps are large enough. Thermally triggered hopping is a phenomenon that explains this movement of electrons and holes at appropriate temperatures. According to this mechanism, the energy gained from the thermal fluctuations inside the lattice causes the electrons and holes to hop between the various traps prior to entering the conduction band. The distance between the various trap locations is crucial since this sort of transportation also requires quantum mechanical tunneling. This will ultimately lead to a conduction of carriers across the polymer, with the conduction rate mostly determined by the depth and distance between neighboring traps rather than the properties of the conduction band.

The extended model of the band-gap, which is a more appropriate description of the energy band with the impact of the traps, can explain why the charge transport varies throughout the material due to the various states/traps. "Shallow-traps" are the traps that are situated at the conduction band's edge. The charges in this area will hop between the various traps, supporting the charge transit. The conduction band is situated at a lower level for this reason. As the charge carriers will be confined to the states for a while before moving on to other states, the mobility of the charge carriers is low in this area. This suggests that the "depth" of the traps, their concentration, and the detrapping process all have a significant impact on their conduction through the insulator. The "deep-traps" are the traps found at lower levels. Because charge carriers are held in these traps for extended periods of time, they will also have an impact on charge transfer. Furthermore, because the density of the deep traps is much lower, there is no hopping between them. As a result, the material will be able to retain charge for a longer period of time and its conductivity will be further decreased by the deep traps.

2.2.3 Macroscopic Expression for Conductivity

Although conduction was discussed from the perspective of charge carriers in the preceding section, we will now provide a macroscopic expression for conductivity and consider the causes of its dependence. The Klein's conductivity expression for the bulk conductivity, with electric field and temperature dependency, is:

$$\sigma = \sigma_0 e^{\alpha T} e^{\beta E} \tag{2.4}$$

where σ_0 is the conductivity without temperature and field dependency, T is the temperature expressed in its measured unit, α [1/°C] and β $[(kV/mm)^1]$ are constants and E is the electric field in [kV/mm].

The temperature and field dependency originates from the expression for the

hopping conduction, From the expression it can be realised that the conduction, due to the hopping mechanism in the shallow traps, have an exponential temperature and field dependency. Additionally, trapping and detrapping to deep traps also feature strong field and temperature dependencies. It is evident that the macroscopic conductivity equation thus is the sum of all the conduction processes occurring within the material.

2.2.4 Reducing the By-product Content in the Polymer

As mentioned in section 2.1.2, dicumyl peroxide is utilized as a catalyst in the vulcanization procedure in order to create the precise chemical composition required for cross-linked polyethylene. When dicumyl peroxide is used as a catalyst, residues are produced in the specimen, including methane, alfa-methylstyrene, cumyl alcohol, and acetophenone [11]. By altering the impurity rate and, consequently, the concentration of traps in the energy gap, these undesirable byproducts have an effect on conductivity. This suggests that the conductivity rises as the catalyst's byproducts increase. Furthermore, after ionization, these residues may move throughout the material and raise conductivity once more. The insulation material can be treated to a temperature below T_m, which enables quicker outgassing of these residues, to lower the impurity level and minimize the effect on conductivity. This procedure, also known as degassing, is carried out following the HVDC cable's extrusion process. This step is carried out because the outgassing that occurs during the extrusion process alone is insufficient to minimize the impurity content during later electrical screening tests. The byproducts will continue to evaporate throughout the subsequent degassing procedure, but this will also increase the specimen's crystallinity. This is because the tiny crystals formed during the cooling of the material following cross-linking will melt and mix with other crystals. As a result, during the reheating process, larger crystals will form, increasing the crystallinity. The growth rate of bigger crystals near the melting temperature during a specific time period can be further explained by this phenomenon, known as thermal annealing. This suggests that specimens that undergo different degassing procedures may have distinct morphological structures and residue contents, which could affect conductivity.

3

Methodology: Test setup and procedure

This project aims to ensure a stable test setup that works for many samples and to perform measurements with accurate results. As a result, the primary focus of this thesis has been the test procedure.

3.1 Cable Peelings

The electrical tests performed during this project consisted of the comparison of the leakage current within cable insulation peeling samples.

The cable peelings were provided from Nexans Norway. An HVDC cable's extrusion process is carried out automatically in huge quantities, which may cause a small variation in the circumference of the cable. This variance may cause the extracted cable peeling to have varying thicknesses along its lengthwise orientation. A paint depth gauge was utilized to measure the thickness in order to improve accuracy and lower these uncertainties. The thickness was measured after all electrical testing were finished to reduce the possibility of the samples' surfaces being harmed.

Cable peelings are cut from 3 different positions in the insulation (inner, middle and outer), in the appropriate shape and size and marked to distinguish between samples taken from different positions. Since the electrodes are of 10 cm diameter, the peeling samples were cut to be at least 16 cm. This gives a room of 3 cm on all sides of the electrode to decrease the chances of electrical breakdown by increasing the creepage distance. The polymeric samples absorb moisture from the surrounding air when they are in a humid environment until they reach equilibrium. The sample absorbs more water when the surrounding humidity is higher. It is very challenging to remove the water content from the sample. Therefore,

the samples are kept in a sealed tank with silica gel to speed up the drying process before subjecting them to reduced humidity conditions. The extremely low relative humidity of 10% inside the tank is provided by the silica gel, which absorbs water.

3.2 Test set-up

3.2.1 Temperature and humidity conditions

In order to control temperature, measurements are run inside the laboratory climate chamber. This oven is also able to control humidity, which is set to 0% relative humidity.

3.2.2 Conductivity measurements

Electrical conductivity of the samples is determined by measuring the electric resistance of a material and taking into account its geometry.

The electrometer 6517B from Keithley depicted in Figure 3.1 is used in conjunction with a voltage source to apply voltages of 3 kV, 6 kV and 9 kV, and measure the current which is in the pico ampere range. A LabVIEW program interfaces with the device and allows for data retrieval.

Figure 3.1: *Testing setup of electrometer, channel selector, and voltage source.*

Since the electrometer's initial current reading incorporates capacitive and polarization components, it cannot be utilized to calculate conductivity. It is estimated that the current passing through the polymer sample will decrease rapidly until, in a steady state, it is only conduction current. A compromise was reached, and

4 hours was selected as the measuring period because it would take too long for the samples evaluated in this study to attain what may be called a steady state.

A single conductivity value was obtained by averaging the last 200 current readings for each sample (the standard sampling rate is 10 samples per second). The coefficient of variation of those 200 readings divided by their average value is the measure of uncertainty called **the standard deviation percentage.**

3.2.3 Electrodes

The electrode and guard are separated by a gap of approximately a tenth of a millimeter. The spacing distance is maintained with polyamide tape. The purpose of the guard electrode is to eliminate the surface leakage currents.

A channel selector, seen in Figure 3.1, which functions as a multiplexor to enable the simultaneous performance of four measurements, is utilized to expedite the testing. The analog signal being recorded by the electrometer is constantly altered by the multiplexor by selecting one of the four channels. Each sample type is tested twice at the same time, and two samples are measured concurrently. Two bottom electrodes and four top electrodes are needed for this arrangement. The whole arrangement can be seen in Figure 3.2.

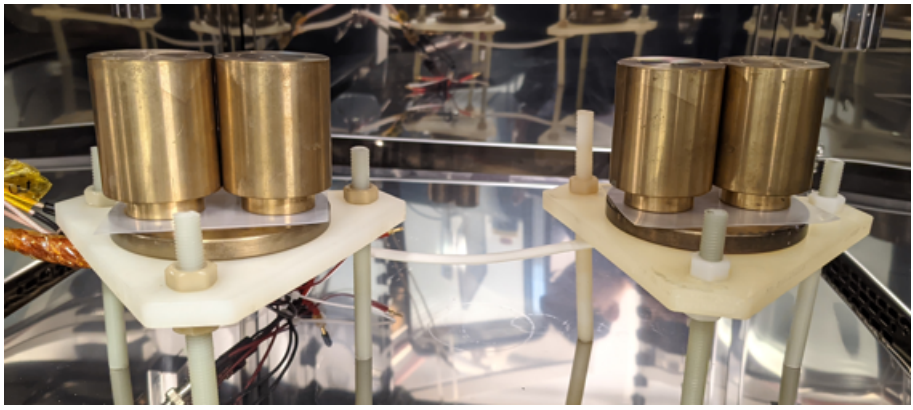

Figure 3.2: *The HV and LV electrodes' setup*

The bottom electrodes are coupled to the electrometer's high voltage side via an HV wire and a resistor, for protection against faults. Coaxial cables are used to link the electrometer to the top electrodes. The outward portion of the wire is attached to the guards, while its interior is connected to electrodes. The cable's outward portion is at ground potential.

3.3 Testing Procedure

The components and their functions have been discussed in detail in the preceding sections. We will now go over the specifics of the tests conducted on the samples. The high voltage and low voltage electrodes, which are situated in a climate chamber, will be sandwiched between each sample (cable peeling).

Every single sample has to be tested for eight hours, which will be split equally between two time intervals of four hours each. The first will be used to heat the samples to the necessary temperature, and the second will use a voltage level of 3, 6, or 9 kV, depending on the test being conducted. This test will be performed within the climate chamber and at three different temperature levels; 20°C, 50°C and 70°C, although, the samples were tested at 50°C first so as to soften them slightly and form a better contact patch with the electrodes. Thus, the testing order was 50°C, then 20°C, and finally 70°C.

In total there were 36 peeling samples tested, across 3 different temperatures and 3 different voltage levels and 2 different thicknesses.

4

Results and Discussions

4.1 Impact of Temperature

The first test was run to see the effects of temperature on the cable peelings. For this, the peelings were placed between two electrodes with a potential difference of 3 kV. For an average peeling thickness of 300 µm, this gives us an electric field of 10 kV/mm. The test was run for 4 hours, after which the readings of the leakage currents of each sample was noted down, and subsequently, the electrical conductivity of each sample was calculated. The electrical conductivity readings of each sample is shown in Table 4.1 and graphically represented in Figure 4.1.

From the data, a few observations can be made. The most important one being that the conductivity rises as the temperature is increased. This matches with what we had expected, based on the literature of the macroscopic conductivity expression.

The second observation is that, as the temperature is increased, the standard deviation of the conductivity reading decreases. This can be attributed to the fact that at low temperatures, the leakage current is significantly lower than that at high temperatures (roughly by a factor of 10). This low leakage current is harder for the electrometer to detect accurately, thus resulting in the average leakage current having higher standard deviation. As the temperature increases, the leakage current of the peeling increases, which is detected more accurately by the electrometer. This results in lower standard deviations for the average value of leakage current.

Table 4.1: *Electrical conductivity readings for the different samples.*

			20°C	50°C	70°C
Inner Peelings	Sample 1	Conductivity	3.71E-16	4.21E-15	2.04E-14
		Stan. Dev. %	171%	228%	129%
	Sample 2	Conductivity	2.35E-16	4.20E-15	5.44E-14
		Stan. Dev. %	263%	279%	163%
	Sample 3	Conductivity	4.22E-16	6.81E-15	1.65E-14
		Stan. Dev. %	157%	216%	191%
	Sample 4	Conductivity	1.81E-16	4.57E-15	1.05E-14
		Stan. Dev. %	123%	190%	66%
	Average Conductivity		3.02E-16	4.95E-15	2.55E-14
Middle Peelings	Sample 1	Conductivity	5.71E-16	3.52E-15	2.20E-14
		Stan. Dev. %	221%	183%	338%
	Sample 2	Conductivity	2.55E-16	4.56E-15	2.77E-14
		Stan. Dev. %	219%	197%	348%
	Sample 3	Conductivity	5.06E-16	3.65E-15	1.90E-14
		Stan. Dev. %	143%	149%	158%
	Sample 4	Conductivity	4.35E-16	2.93E-15	3.54E-14
		Stan. Dev. %	181%	239%	28%
	Average Conductivity		4.42E-16	3.66E-15	2.60E-14
Outer Peelings	Sample 1	Conductivity	1.15E-15	6.83E-15	1.88E-14
		Stan. Dev. %	158%	178%	140%
	Sample 1	Conductivity	3.53E-16	4.07E-15	8.98E-15
		Stan. Dev. %	227%	223%	57%
	Sample 1	Conductivity	1.91E-16	2.87E-15	3.79E-14
		Stan. Dev. %	143%	170%	68%
	Sample 1	Conductivity	7.37E-16	2.44E-15	1.59E-14
		Stan. Dev. %	109%	86%	53%
	Average Conductivity		6.07E-16	4.05E-15	2.04E-14

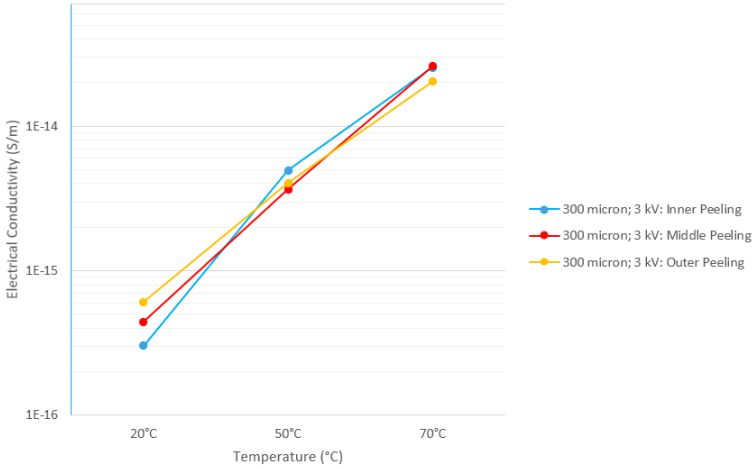

Figure 4.1: *Graphical representation of the average conductivity values.*

4.2 Impact of Peeling Thickness

Next, the effect that the peeling thickness itself might have on the conductivity readings is tested. For this, the samples of 600 µm average thickness were tested under the same electric field as the 300 µm samples, i.e. 10 kV/mm. This was achieved by increasing the potential difference between the electrodes to 6 kV. Since the electric field and temperature in both the tests are the same, these variables can be isolated from the readings, and we can safely say that any change in the conductivity readings will be caused by the difference in the peelings' thickness. The conductivity readings for each 600 µm sample is shown in Table 4.2 and a graphical comparison between the 300 µm and 600 µm samples is shown in Figure 4.2.

The key observation here is that the conductivity readings for the 600 µm samples is significantly lower than that of the 300 µm samples. This can be attributed to two factors, space charges and presence of by-products in the peelings. Since the 600 µm samples are twice as thick as the 300 µm samples, there will be a higher degree of space charges in them. This results in a lowering of the electrical conductivity of the peeling samples.

A similar thing can be said about the polyethylene by-products. An increased thickness means a higher presence of the polyethylene by-products in the samples, and as we have seen in the literature review chapter, this increases the electrical conductivity of the sample.

Table 4.2: *Electrical conductivity readings for the different samples at 6 kV.*

			20°C	50°C	70°C
Inner Peelings	Sample 1	Conductivity	1.60E-16	9.39E-16	3.02E-15
		Stan. Dev. %	105%	107%	28%
	Sample 2	Conductivity	5.08E-16	4.04E-15	8.31E-15
		Stan. Dev. %	186%	30%	18%
	Sample 3	Conductivity	3.32E-16	8.30E-16	4.00E-15
		Stan. Dev. %	216%	212%	53%
	Sample 4	Conductivity	2.56E-16	6.40E-16	3.93E-15
		Stan. Dev. %	250%	169%	37%
	Average Conductivity		3.14E-16	1.61E-15	4.82E-15
Middle Peelings	Sample 1	Conductivity	6.32E-16	9.15E-16	9.80E-16
		Stan. Dev. %	176%	122%	116%
	Sample 2	Conductivity	1.42E-16	4.39E-16	9.11E-16
		Stan. Dev. %	270%	144%	123%
	Sample 3	Conductivity	1.41E-16	3.93E-16	1.75E-15
		Stan. Dev. %	167%	118%	88%
	Sample 4	Conductivity	2.52E-16	3.66E-16	1.67E-15
		Stan. Dev. %	118%	139%	191%
	Average Conductivity		2.92E-16	5.28E-16	1.33E-15
Outer Peelings	Sample 1	Conductivity	2.31E-16	5.45E-16	1.45E-15
		Stan. Dev. %	201%	133%	27%
	Sample 1	Conductivity	2.96E-16	4.86E-16	1.36E-15
		Stan. Dev. %	148%	112%	31%
	Sample 1	Conductivity	1.81E-16	1.23E-15	3.87E-15
		Stan. Dev. %	250%	162%	38%
	Sample 1	Conductivity	1.61E-16	9.97E-16	1.56E-15
		Stan. Dev. %	149%	105%	105%
	Average Conductivity		2.17E-16	8.15E-16	2.06E-15

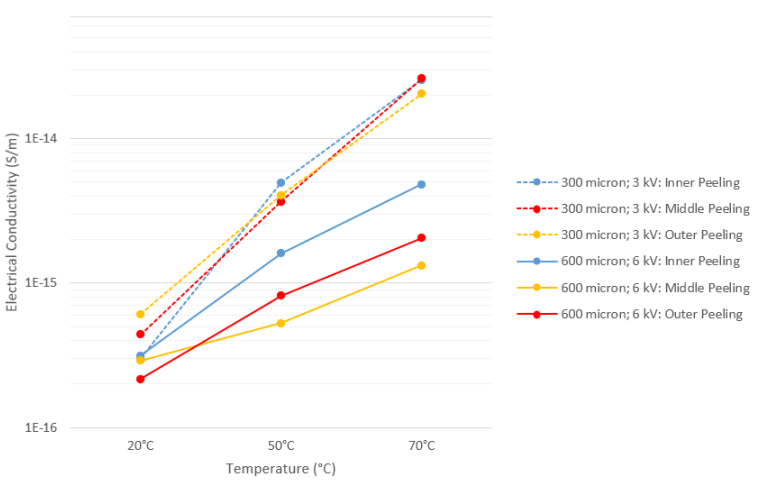

Figure 4.2: *Graphical representation comparing the average conductivity values of the 300 µm and 600 µm samples.*

4.3 Impact of Electric Field

The 300 µm samples were tested again, but under a higher electric field of 30 kV/mm. For this, the potential difference between the electrodes was increased to 9 kV. The conductivity readings for each sample is shown in Table 4.3 and a graphical comparison between the 3 kV and 9 kV data is shown in Figure 4.3.

From the graph, it is very evident that the increase in electric field has caused the electric conductivity to increase as well. Again, this follows from what we studied in the 'Macroscopic Conductivity Expression' section in the literature review chapter.

On comparing the conductivity readings for the samples tested at 3 kV and 9 kV concurrently for each test temperature, we can make another quick observation that a change in temperature has a higher impact on the conductivity readings than a change in the electric field. This means that, for the Klein's expression of electrical conductivity studied in the literature review chapter, the temperature coefficient will be greater than the electric field coefficient. The exact value of these coefficients will be calculated in a later section, when the data obtained through testing will be used to create a COMSOL model of the HVDC cable.

4.4 Impact of Peeling Position

Another objective of this project, was to study the effect that the position from which the peelings were taken (i.e. inner, middle or outer part of the cable insulation) will have on the overall conductivity readings. For this, samples from all

Table 4.3: *Electrical conductivity readings for the different samples at 9 kV.*

			20°C	50°C	70°C
Inner Peelings	Sample 1	Conductivity	2.31E-15	9.21E-15	3.69E-14
		Stan. Dev. %	33%	24%	89%
	Sample 2	Conductivity	1.50E-15	5.65E-15	4.32E-14
		Stan. Dev. %	132%	33%	126%
	Sample 3	Conductivity	3.44E-15	8.48E-15	3.41E-14
		Stan. Dev. %	32%	40%	60%
	Sample 4	Conductivity	2.61E-15	7.14E-15	3.45E-14
		Stan. Dev. %	23%	50%	53%
	Average Conductivity		2.47E-15	7.62E-15	3.72E-14
Middle Peelings	Sample 1	Conductivity	9.98E-17	5.36E-15	2.58E-14
		Stan. Dev. %	252%	60%	28%
	Sample 2	Conductivity	2.37E-16	5.36E-15	3.23E-14
		Stan. Dev. %	214%	13%	78%
	Sample 3	Conductivity	1.70E-16	6.64E-15	4.53E-14
		Stan. Dev. %	300%	174%	43%
	Sample 4	Conductivity	6.76E-17	5.33E-15	3.08E-14
		Stan. Dev. %	183%	38%	12%
	Average Conductivity		1.44E-16	5.67E-15	3.35E-14
Outer Peelings	Sample 1	Conductivity	2.65E-16	4.17E-15	5.10E-14
		Stan. Dev. %	98%	28%	64%
	Sample 1	Conductivity	1.22E-16	5.06E-15	3.55E-14
		Stan. Dev. %	224%	24%	32%
	Sample 1	Conductivity	8.19E-17	1.29E-14	4.96E-14
		Stan. Dev. %	318%	49%	21%
	Sample 1	Conductivity	8.15E-17	1.14E-14	4.92E-14
		Stan. Dev. %	303%	38%	19%
	Average Conductivity		1.38E-16	8.40E-15	4.63E-14

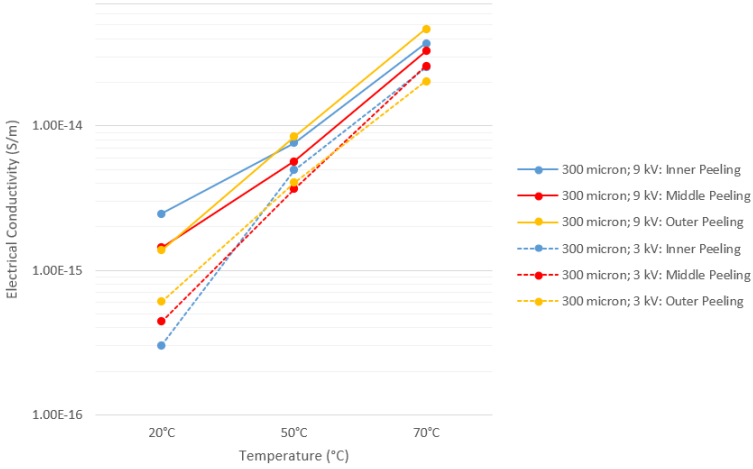

Figure 4.3: *Graphical representation comparing the average conductivity values of the samples at different electric fields.*

the 3 positions in the cable insulation were tested, as can be seen from the data in the previous sections.

It is observed that there is some evidence to suggest that electrical conductivity will be lowest in the middle of the cable insulation, irrespective of the operating temperature or voltage of the HVDC cable. However, at some of the data points, this does not seem to be the case as well. This is probably because of two factors: variation in the peelings' thickness and high standard deviation of the electric conductivity readings. Since all the cable peeling samples, even within the same test, have slightly different thicknesses due to tolerances in the machine used to make the peelings, the electric field of each sample is slightly different. This results in a somewhat "apples to oranges" comparison of each sample, since electrical conductivity is ultimately dependent on the electric field as well. The fact that the low leakage current levels result in high standard deviation values of the conductivity readings only exacerbates this issue.

Since neither of these two factors can be accounted for, or isolated in the tests done for this project, further testing will be required to confirm the hypothesis made in this section.

5

Computational Modeling of HVDC Cable

Once the testing was completed, and all the data compiled and analysed, we performed curve fitting on MATLAB to find a correlation between electrical conductivity, temperature, and electric field. This expression will then be used to create a model for analysing electric field distributions in the HVDC cable under load.

5.1 Computational Model

5.1.1 Mathematical Description

For the modelling, Comsol Multiphysics software was used. Two coupled physical interfaces were adopted, specifically, Electric Current (ec) and Heat Transfer in Solids (ht).

Electric Current physics makes use of the differential form Gauss' law in the Maxwell equations, given by:

$$\nabla \cdot J = 0 \tag{5.1}$$

where J refers to the current density

Also, electric field as the gradient of potential is given as:

$$E = -\nabla \cdot V \tag{5.2}$$

where V is the potential.

The electric displacement field D is related to the electric field as:

$$D = \epsilon_0 \epsilon_r E \tag{5.3}$$

where ϵ_0 and ϵ_r are the vacuum and relative permittivity, respectively.

We also make use of Ohm's Law, given by:

$$J = \sigma(T) \cdot E \tag{5.4}$$

Here, σ refers to the electrical conductivity that is dependent on temperature.

Heat Transfer physics, which is used to implement temperature variations in the cable under different load conditions, makes use of the Fourier's Law, given by:

$$q = -k\nabla T \tag{5.5}$$

Here, q refers to the heat flux vector, k refers to the thermal conductivity of the medium, and T refers to the temperature.

The Heat Transfer in Solids Interface solves for the following equation:

$$\rho C_p \left(\frac{\partial T}{\partial t} \right) + \nabla q = Q \tag{5.6}$$

where ρ is the density of the insulation layer, C_p is the specific heat capacity at constant stress, and Q denotes an external heat source, used to model the ohmic losses in the conductor.

Thus, we can then define electric conductivity in COMSOL as a function of the variables temperature and electric field, as given by Klein's conductivity expression for bulk conductivity (equation 2.4).

5.1.2 Problem Implementation

Assuming that the cross-section of the cable is the same along its entire length, one may consider a 2D approximation and implement the cross-section of the cable in COMSOL with the properties discussed henceforth.

Application and study: Electric Current (ec) and Heat Transfer in Solids (ht) physics, and Electromagnetic Heating multiphysics study in Time Dependent mode. The range of time is taken as 0 minutes to 1500 minutes. Since the electrometer's initial current reading incorporates capacitive and polarization components that last for a very short amount of time, the time range is divided as follows:

	Initial Value (minutes)	Final Value (minutes)	Time Step (minutes)
Range 1	0	5	0.5
Range 2	5	100	1
Range 3	100	1500	10

Mesh properties: we have used the following user-controlled mesh to gain fine-grained control over the mesh elements near the conductor for better accuracy and efficiency. Since the solution does not change as quickly in the other parts of the insulation, a coarser mesh can be used to reduce the computational time and memory.

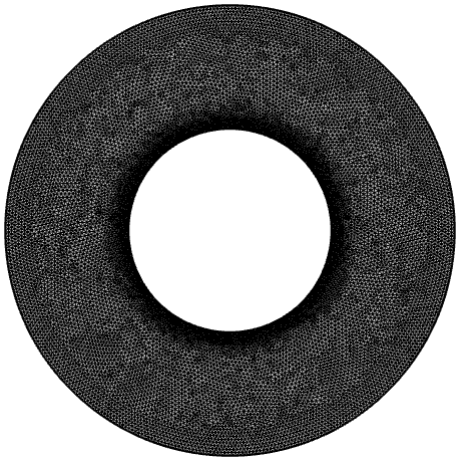

Figure 5.1: *Mesh Properties*

The following electrical and thermal parameter values were used:

Name	**Value**
Relative permittivity	2.3
Ohmic losses	100 W
Thermal conductivity	0.3 W/(m.K)
Density	920 kg/m^3
Heat capacity at constant pressure	1900 J/(kg.K)

5.2 Results and Discussion

Before the COMSOL model could be created, a curve fitting exercise was carried out in MATLAB using the data obtained from the previous tests, to obtain the values of the temperature coefficient and electric field coefficient. An 'exponential' fit type was used, since it gave the best values of R^2, also known as the coefficient of determination, which is a statistical term that measures how much of the variability in a dependent variable (in this case, electrical conductivity) can be explained by an independent variable (in this case, temperature and electric field).

The results from curve fitting can be seen in the following table, and in Figure 5.2, comparing it with the readings from the tests.

	Values	R^2
$sigma_0$	1.28e-17	-
alpha	0.119	0.9428
beta	9.195e-2	1

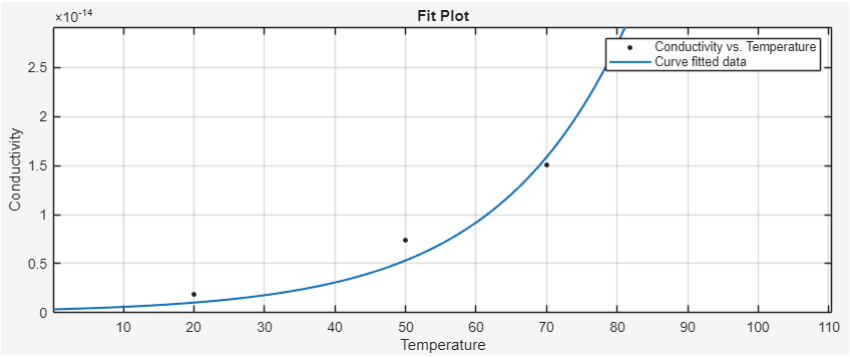

Figure 5.2: *Comparison between curve fitting plot and electrical conductivity readings from tests.*

These values were then used to create a COMSOL model of the HVDC cable, and the electric field inside the cable insulation was observed for 1500 minutes.

It was observed that the electric field was higher on the inner part of the insulation initially, which is similar to the electric field distribution in an HVAC cable. However, at the end of 1500 minutes, it was observed that the field distribution had reversed, and now the outer part of the insulation was exposed to higher electric fields. This phenomenon is known as 'field inversion' and is shown in Figure 5.8. This happens due to the development of a temperature gradient inside the insulation layer of a cable that is under load. With time, the ohmic losses from the conductor heat up the insulation layer, resulting in a higher temperature gradient, as seen in Figure 5.2 and 5.3. The hotter inner insulation layer becomes more conductive, while the cooler outer insulation layer stays less conductive. This results in the generation of space charges in the inner parts of the insulation, which then migrate and accumulate midway through the insulation layer. The space charge density generated over the same period of time due to this phenomenon can also be seen in Figure 5.4 and 5.5. This accumulation of space charges, in turn causes the electric field inside the insulation to 'invert', which results in the outer insulation layer being at a higher electric field than the inner insulation layer, as seen in Figures 5.6 and 5.7.

This phenomenon is important to keep in mind while designing the insulation

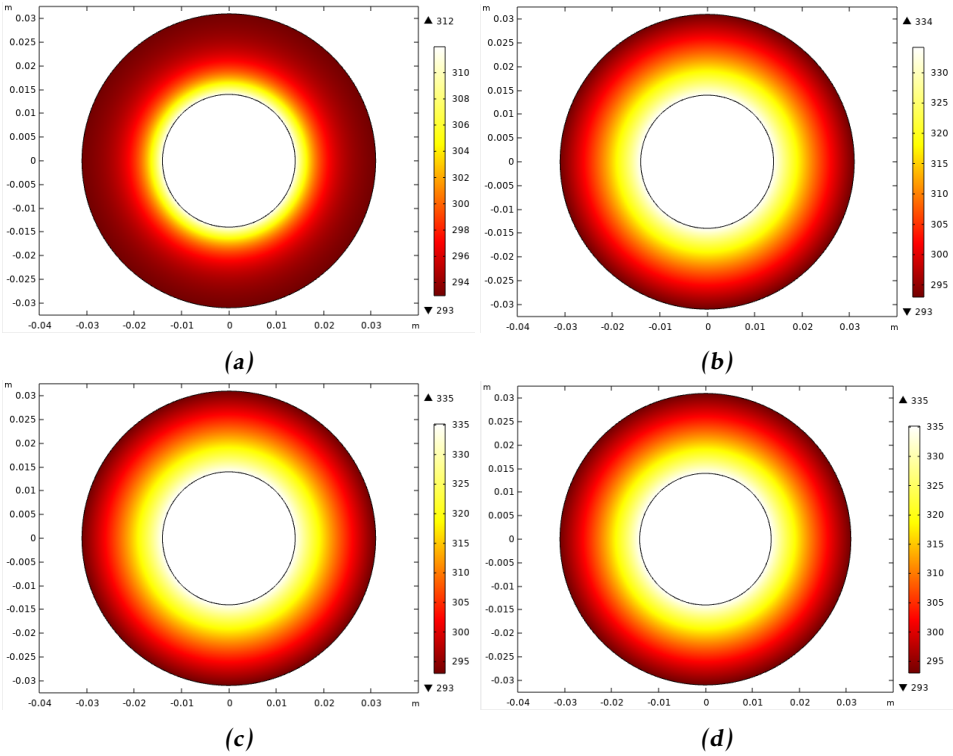

Figure 5.3: *Temperature gradient inside the cable insulation at (a) 0 minutes, (b) 30 minutes, (c) 100 minutes, and (d) 1500 minutes.*

layer of an HVDC cable, since the outer insulation layer needs to be designed in such a way that it can sustain the higher electric fields that it will be subject to after deployment. Also, since field inversion occurs due to the formation of a temperature gradient in the insulation layer, its effects can be reduced by increasing the thermal conductivity of the insulating material by mixing in additives during the manufacturing process.

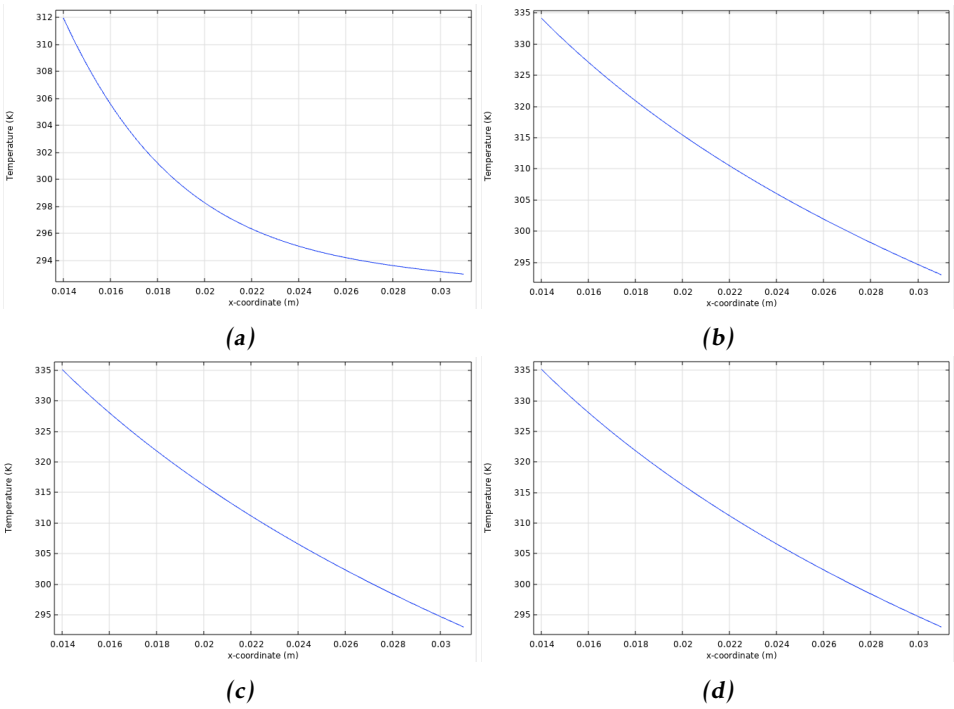

Figure 5.4: *Graphical representation of temperature gradient inside the cable insulation along its radius at (a) 0 minutes, (b) 30 minutes, (c) 100 minutes, and (d) 1500 minutes.*

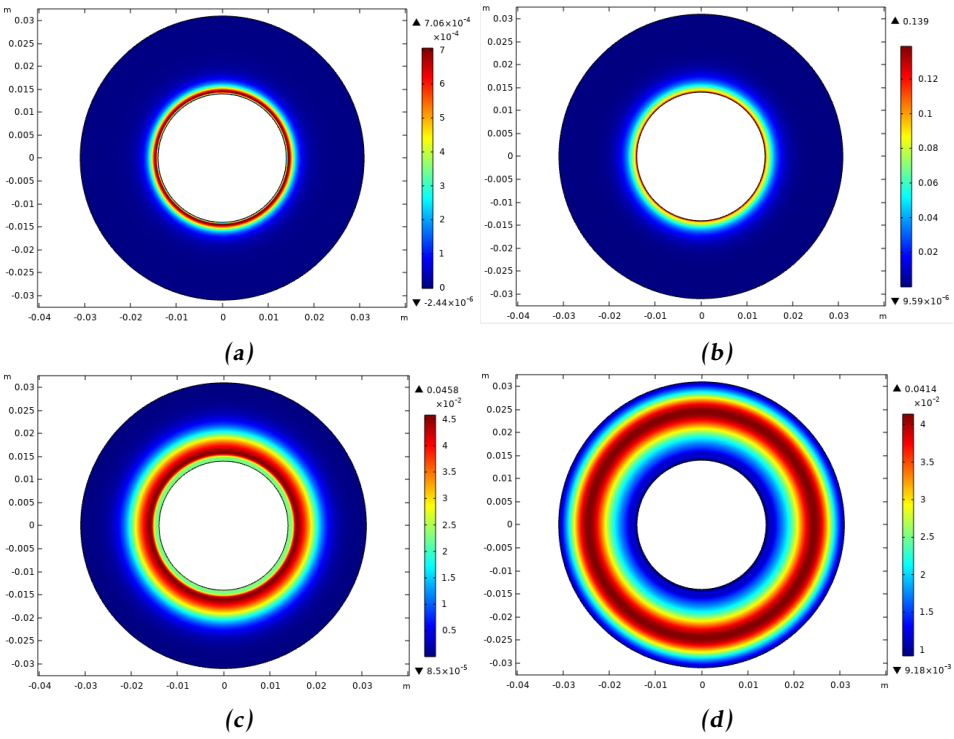

Figure 5.5: *Space charge density inside the cable insulation at (a) 0 minutes, (b) 30 minutes, (c) 100 minutes, and (d) 1500 minutes.*

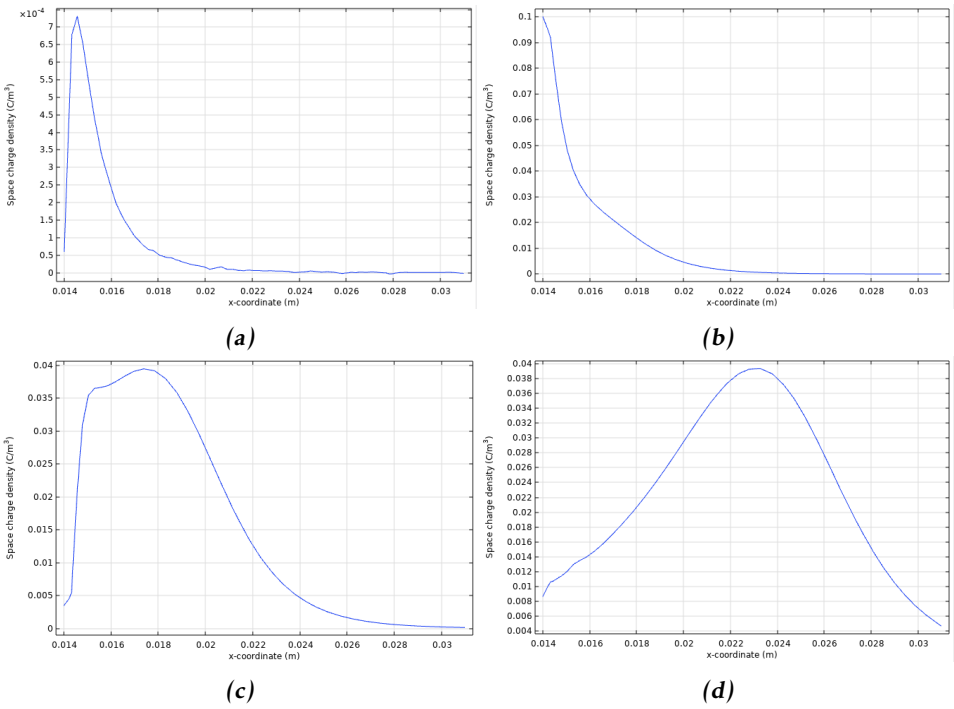

Figure 5.6: *Graphical representation of space charge density inside the cable insulation along its radius at (a) 0 minutes, (b) 30 minutes, (c) 100 minutes, and (d) 1500 minutes.*

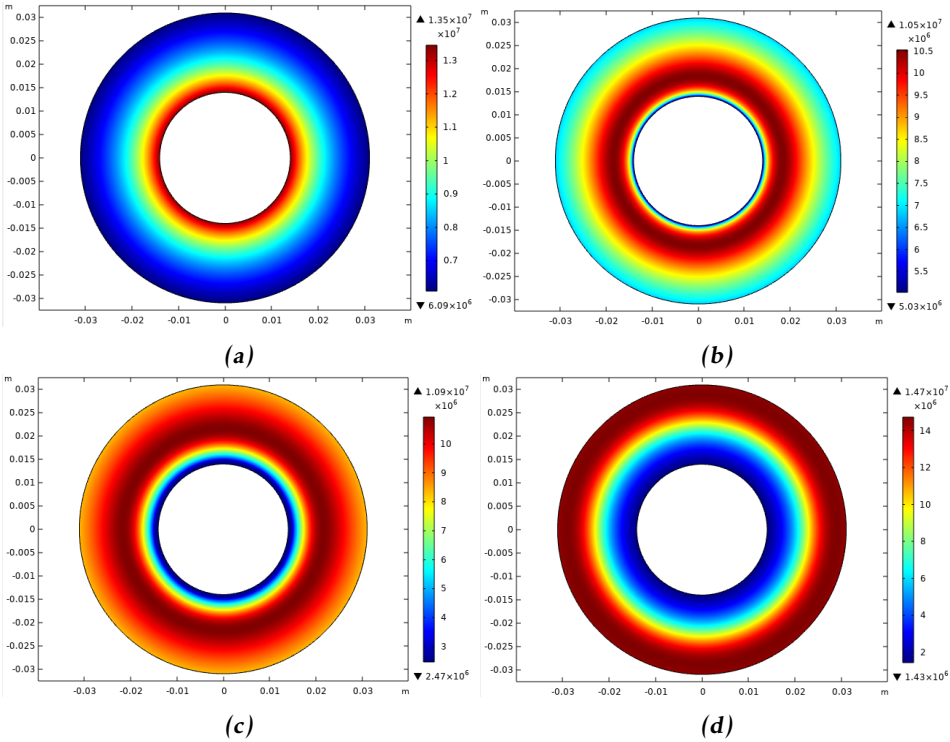

Figure 5.7: *Electric field inside the cable insulation at (a) 0 minutes, (b) 30 minutes, (c) 100 minutes, and (d) 1500 minutes.*

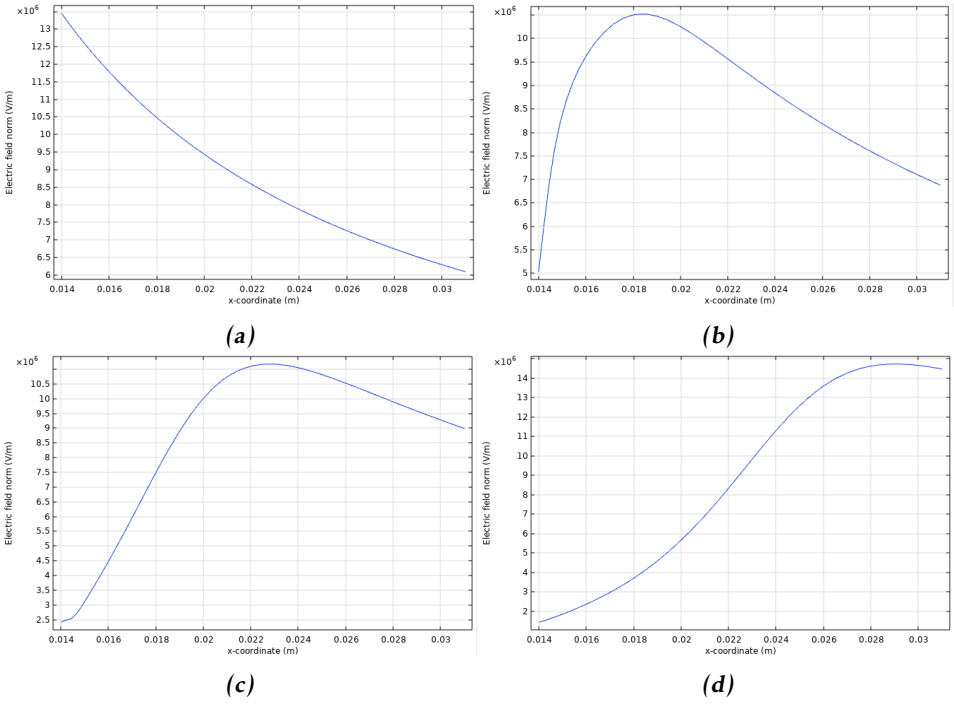

Figure 5.8: *Graphical representation of electric field distribution inside the cable insulation along its radius at (a) 0 minutes, (b) 30 minutes, (c) 100 minutes, and (d) 1500 minutes.*

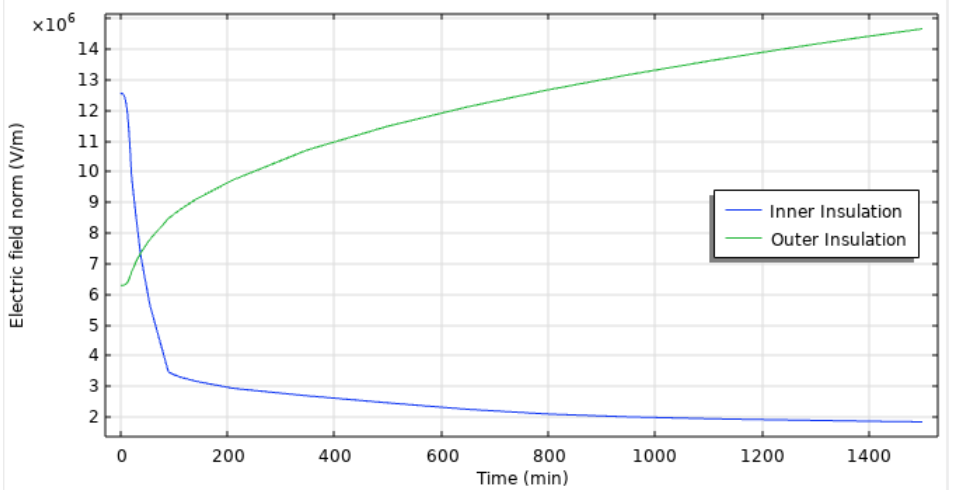

Figure 5.9: *Graphical representation of electric field inversion at two points in the cable insulation (inner and outer) from 0 to 1500 minutes.*

6

Conclusion

The aim of the thesis was to study the electrical conductivity in HVDC cables, by analysing the different parameters that might have an effect on it. These parameters are: temperature, humidity, electric field and presence of XLPE by-products. Out of these, only the effects of temperature and electric field were studied in this project as these are of higher significance to the industry.

Since we measured the electrical conductivity on peelings taken from the cable insulation, it was also studied if the thickness of the peelings will have an impact on the conductivity readings. Also, since the by-product content is not the same throughout the insulation after the degassing process, it was also studied if the position the peeling was taken from will have an effect on the conductivity readings.

A test setup was created with 4 measurement electrodes setup, an electrometer, and a channel selector. The readings from the electrometer were recorded in a computer that was configured with a LabView program developed in the university department to calculate the electrical conductivity of materials.

First, a test was conducted to study the impact of temperature on the electrical conductivity. It was observed that as the temperature increases, the conductivity increases exponentially as well. It was also observed that an increase in temperature resulted in a decrease in the standard deviation of the conductivity readings. This effect was concluded to be due to the increase in leakage current with increase in temperature, making the conductivity readings more accurate.

After this, the effect of the peelings' thickness on conductivity was studied by comparing the conductivity values of a 300 μm and a 600 μm insulation peelings.

It was found that the thicker peelings had a lower electrical conductivity. This can be explained by the increased space charges, that develop in insulations under HVDC loads. A thicker peeling will have a higher number of space charges, and thus, a lower electrical conductivity.

Then, we studied the effects of electric field on conductivity. For this, the 300 µm peelings were tested by increasing the potential difference between the electrodes to 9 kV, thereby giving an electric field of 30 kV/mm. Here, the observation was that conductivity increased with an increase in electric field as well, but not as much as it did with an increase in temperature. The standard deviation values seemed to reduce here as well. This was also concluded to be due to the increased leakage current caused by a higher electric field.

Finally, all the data from the previous tests were studied concurrently to determine the effect of the peelings' position on conductivity. Although there was some evidence to suggest that conductivity would be lower if the peelings are taken from the middle of the insulation, due to uncontrollable parameters like inconsistencies in peeling thickness and by-product concentration, and very high standard deviation in the readings, a conclusive explanation could not be provided.

The data from all the tests was then used to perform a curve fitting exercise on MATLAB to get the relation between temperature, electric field and electrical conductivity. Since the 'exponential' fit type gave the best values of R^2 for the temperature and electric field coefficients, it was concluded that Klein's expression of conductivity was the best fit for the test data.

After this, a model of an HVDC cable was created in COMSOL using the coefficient values, obtained from curve fitting. It was observed that due to the development of a temperature gradient in loaded HVDC cables, over time, the electric field distribution in the insulation 'inverts', from being higher on the inner part initially, to being higher on the outer part as the temperature gradient in the insulation layer increases. This effect is known as 'field inversion'.

Thus, all the parameters that we aimed to study were analysed and their effects were also observed on a loaded HVDC cable model.

7

Bibliography

[1] E. E. Peschke and R. v. Olshausen, Cable systems for high and extra-high voltage : development, manufacture, testing, installation and operation of cables and their accessories. Publicis MCD Vlg, 1999.

[2] E. Doedens, "Characterization of Different Interface Types for HVDC Extruded Cable Applications," Ph.D. dissertation, 2018. [Online].
Available: https://research.chalmers.se/publication/502706

[3] Tektronix, "Model 6517B Electrometer Reference Manual," Tech. Rep., 2016. [Online]. Available: https: //www.tek.com/keithley-low-level-sensitive-and-specialty-instruments/ keithley-high-resistance-low-current-electr-0

[4] T. Worzyk, Submarine power cables : design, installation, repair, environmental aspects. Springer, 2009.

[5] "Fundamentals of HVDC Cable Transmission," in Extruded Cables For High-Voltage Direct-Current Transmission. Hoboken, New Jersey: John Wiley Sons, Inc., 6 2013, pp. 11–40. [Online].
Available: http: //doi.wiley.com/10.1002/9781118590423.ch02

[6] T. Worzyk, Submarine Power Cables, ser. Power Systems. Berlin, Heidelberg: Springer Berlin Heidelberg, 2009.

[7] R. Ross and W. Geurts, "Application of polyethylene sheath and swelling powder against water treeing," in ICSD'98. Proceedings of the 1998 IEEE 6th International Conference on Conduction and Breakdown in Solid Dielectrics (Cat. No.98CH36132). IEEE, pp. 345–348. [Online].

Available: http://ieeexplore.ieee.org/document/709296/

[8] "Plastics-the Facts 2017 An analysis of European plastics production, demand and waste data," Tech. Rep. [Online].
Available: https://www.plasticseurope.org/application/files/5715/1717/4180/Plastics-the-facts-2017-FINAL-for-website-one-page.pdf

[9] N. G. McCrum, C. P. Buckley, and C. B. Bucknall, Principles of polymer engineering. Oxford University Press, 1997.

[10] F. Zhou, J. Li, Z. Yan, X. Zhang, Y. Yang, M. Liu, D. Min, and S. Li, "Investigation of charge trapping and detrapping dynamics in LDPE, HDPE and XLPE," IEEE Transactions on Dielectrics and Electrical Insulation, vol. 23, no. 6, pp. 3742–3751, 12 2016.

[11] L. A. Dissado and J. C. Fothergill, Electrical Degradation and Breakdown in Polymers. The Institution of Engineering and Technology, Michael Faraday House, Six Hills Way, Stevenage SG1 2AY, UK: IET, 1 1992.

[12] C. C. Ku and R. Liepens, Electrical Properties of Polymers - Chemical Principles. Münich: Carl Hanser Verlag, 1987.

[13] B. Lee, "Electrical conductivity of carbon black filled polymers—effects of morphology and processing," Journal of Vinyl Technology, vol. 15, no. 3, pp. 173– 176, 1993.

[14] Ten-Year network development plan 2020 completing the Map Power System Needs. Accessed September 23, 2025. https://eepublicdownloads.entsoe.eu/tyndp-documents/IoSN2020/200810-IoSN2020mainreport-beforeconsultation.pdf.

[15] G. Chen, T. Tay, A. Davies, Y. Tanaka, and T. Takada, "Electrodes and charge injection in low-density polyethylene using the pulsed electroacoustic technique," IEEE Transactions on Dielectrics and Electrical Insulation, vol. 8, no. 6, pp. 867–873, 2001. [Online]. Available: http://ieeexplore.ieee.org/document/971439/

[16] G. Teyssedre and C. Laurent, "Charge transport modeling in insulating polymers: from molecular to macroscopic scale," IEEE Transactions on Dielectrics and Electrical Insulation, vol. 12, no. 5, pp. 857–875, 10 2005. [Online]. Available: http://ieeexplore.ieee.org/document/1522182/

[17] P. Morshuis, "Interfaces: To be avoided or to be treasured? What do we think we know?" in 2013 IEEE International Conference on Solid Dielectrics (ICSD). IEEE, 6 2013, pp. 1–9. [Online]. Available: http://ieeexplore.ieee.org/document/6619726/

[18] X. Liu and D. W. Schubert, "Influence of the pressure-dependent contact area between electrode and composite surface on the electrical conductivity," Compos-

ite Structures, vol. 136, pp. 414–418, 2 2016.

DEPARTMENT OF ELECTRICAL ENGINEERING
CHALMERS UNIVERSITY OF TECHNOLOGY
Gothenburg, Sweden 2025
www.chalmers.se

CHALMERS
UNIVERSITY OF TECHNOLOGY